PROCEEDINGS OF THE ROYAL SOCIETY A MATHEMATICAL, PHYSICAL & ENGINEERING SCIENCES

Shock-Wave Observations of Rate Constants for Atomic Hydrogen Recombination from 2500 to 7000 $^\circ$K: Collisional Stabilization by Exchange of Hydrogen Atoms

I. R. Hurle, A. Jones and J. L. J. Rosenfeld

Proc. R. Soc. Lond. A 1969 **310**, 253-276
doi: 10.1098/rspa.1969.0074

Proc. Roy. Soc. A. **310**, 253–276 (1969)
Printed in Great Britain

Shock-wave observations of rate constants for atomic hydrogen recombination from 2500 to 7000 °K: collisional stabilization by exchange of hydrogen atoms

By I. R. Hurle, A. Jones and J. L. J. Rosenfeld
'Shell' Research Ltd., Thornton Research Centre, P.O. Box 1, *Chester*

(*Communicated by T. M. Sugden, F.R.S.—Received* 26 *June* 1968—
Revised 2 *October* 1968)

Rate constants for the recombination of atomic hydrogen with hydrogen molecules, hydrogen atoms, and argon atoms as the third bodies are presented in functional form for the range of temperatures from about 2500 to 7000 °K and are critically compared with the results of other workers. The rate constants are evaluated from detailed analyses of spectrum-line reversal measurements of the fall in temperature accompanying dissociation behind shock waves in gas mixtures containing 20, 40, 50 and 60 % of hydrogen in argon.

The rate constants for recombination with hydrogen molecules (k_{-1}) and argon atoms (k_{-3}) fit the equations

$$\log_{10} k_{-1} = 15{\cdot}243 - 1{\cdot}95 \times 10^{-4} T \text{ cm}^6 \text{ mole}^{-2} \text{ s}^{-1},$$

$$\log_{10} k_{-3} = 15{\cdot}787 - 2{\cdot}75 \times 10^{-4} T \text{ cm}^6 \text{ mole}^{-2} \text{ s}^{-1},$$

with a standard deviation of 0·193 in $\log_{10} k_{-1}$. The rate constant for recombination with hydrogen atoms is about ten times larger than these at 3000 °K and shows a steep inverse dependence on temperature ($\sim T^{-6}$) above 4000 °K. Below this temperature the power of this dependence decreases rapidly and there is strong evidence that the value of this rate constant has a maximum around 3000 °K. This behaviour is interpreted on the basis of a process of collisional stabilization by atom exchange, requiring an activation energy around 8 kcal mole^{-1} and taking place under conditions of vibrational adiabaticity.

The over-all results indicate that the assumption of equality between the equilibrium constant and the ratio of the rate constants for dissociation and recombination is valid throughout the region of non-equilibrium dissociation and at all temperatures in the shock waves examined.

1. Introduction

The recombination of atomic hydrogen has been the subject of extensive study in shock-wave, flame, and room-temperature systems. While the flame results are reasonably self-consistent, though perhaps they suffer to some extent from uncertainties concerning the nature of the attendant third body, the current results from shock-wave systems show areas in which considerable doubt exists concerning absolute values of the recombination rate constants even for a particular species as the third body. Bennett & Blackmore (1968) have critically reviewed the room-temperature data, and through their electron spin resonance studies, taken in conjunction with the work of Larkin & Thrush (1965), they have considerably reduced the doubt in that region. However, the picture in the high-temperature régime remains clouded.

This régime has been probed solely by the use of shock tubes, which provide not only absolute values of rate constants but also their dependence on temperature,

albeit successive experiments have the stimulating habit of yielding somewhat varied and controversial temperature-dependencies. Equally controversial discussions have taken place concerning the origin of these dependencies (cf. Miscellaneous contributors 1962), and mainly for such reasons several studies of molecular dissociation have been made in shock tubes since 1960. A general review of these has recently been given by Hurle (1967*a*).

Apart from the wide ranges of experimental temperatures and pressures afforded by their use, shock waves have the ability to produce an environment in which novel collision processes involving three similar atoms offer a fairly frequent, if not the dominant, route to diatomic recombination. In these respects, both Sutton (1962) and Hurle (1967*b*) found evidence that, while the recombination rate of hydrogen atoms with hydrogen molecules as the third body shows a 'normal' inverse temperature-dependence ($\sim T^{-2}$), the three-atom process involving hydrogen atoms as the third body appears considerably more efficient at 3000 °K and exhibits a much stronger dependence on temperature ($\sim T^{-4}$ to T^{-6}) in the range 3000 to 6000 °K. Although there are indications that the temperature-dependence of this rate constant tends towards a more normal value at the lower temperatures, an extrapolation into the flame and room-temperature régimes predicts values which are both improbably large and apparently unconfirmed.

The experimental results of Hurle (1967*b*) were obtained by the spectrum-line reversal method, which affords a precise monitor of the fall in temperature resulting from molecular dissociation behind the shock front. However, the method used to extract the rate constants from these temperature profiles was rather crude and did not fully use the accuracy of the measured profiles; further, it only allowed the evaluation of the set of rate constants at one mean temperature for each shock wave.

Because of these two features and the unexpected behaviour of the rate constant for the three-atom process, we have since carried out more sophisticated and extensive analyses of the temperature profiles. These are reported in the present paper, together with a more comprehensive account of the experimental method.

2. Experimental

The shock tube

The shock tube has a uniform internal diameter of 10·2 cm and comprises a 243·8 cm long driver section and a 670·6 cm long low-pressure section. The latter is formed from two 274·3 cm long sections and a terminal 121·9 cm observation section joined by ring clamps and sealed by 0-rings.

The individual sections were bar-bored from 18/8 stainless-steel billets of diameter 15·24 cm. After rough boring was completed, the wall thickness was reduced to 1·27 cm by turning down the outside, except at the terminal flanges and at intervals of 60·96 cm along the test section, where short raised bands were left; flats were milled on to these and were then drilled to receive the various shock detectors and window mountings. Welds were thus entirely eliminated from the tube. After these

operations all the sections were joined and bored in-line to produce an inner surface free from discontinuities. The surface finish was to within 10^{-5} cm.

The tube has nine shock-front detectors of the thin-film platinum-resistance type, spaced at intervals of 60·96 cm along the final 548·64 cm of the low-pressure section. The outputs of these are mixed with 10^{-5} s marker pulses and displayed on a Tektronix 535 A oscilloscope, the two time bases of which are coupled to give a raster display of variable line number. This method of monitoring the wave speed over the major portion of the tube allows discrimination against shocks showing undue attenuation or acceleration.

An incident-shock observation station is 106·68 cm and a reflected-shock station 0·635 cm from the end plug. Each station comprises three quartz windows and a Kistler PZ7 pressure transducer mounted circumferentially. The windows are tapered and are sealed with Epikote resin to stainless-steel holders. They are 1·27 cm thick and have a 1·27 cm aperture. The pressure transducers are mounted in O-ring supports to avoid acceleration response, and their faces are coated with a film of silicone grease to prevent temperature response. All the tube fittings have identical dimensions to permit their free interchange.

The double-diaphragm method is used to obtain reproducible driver-gas pressures, the small compartment between the two diaphragms being pressurized to one-half the main driver-gas pressure and then vented to initiate the shock. Half-hard aluminium disphragms ranging in thickness from 0·0914 to 0·3175 cm are scribed to provide a range of driver-gas pressures from 100 to 1500 Lb./in.^{2} ($6{\cdot}7 \times 10^5$ to $1{\cdot}03 \times 10^7$ N m^{-2}). Cold hydrogen and helium are used as the driver gases.

Gas handling and purity levels

The tube was evacuated to 10^{-5} Torr ($1{\cdot}33 \times 10^{-3}$ N m^{-2}) by an Edwards E04 oil-diffusion pump backed by a two-stage rotary pump. The driver section was rough-pumped with a single-stage rotary pump before being filled with the driver gas.

Hydrogen of 99·99 % purity and argon of 99·995 % purity were mixed at 1 atm (101·325 kN m^{-2}) in a stainless-steel stirred vessel, and the mixture was led into the tube through an acetone/carbon dioxide cold trap to avoid any possibility of water contamination. Initial test-gas pressures ranging from 5 to 20 Torr ($6{\cdot}7 \times 10^2$ to $2{\cdot}7 \times 10^3$ N m^{-2}) of 20, 40, 50 and 60 % hydrogen in argon were employed.

Because of the weldless construction of the tube and its large volume ($\sim$ 50l.) there was no measurable leak rate. An outgassing pressure rise of about $1{\cdot}7 \times 10^{-6}$ Torr s^{-1} ($2{\cdot}2 \times 10^{-4}$ N m^{-2} s^{-1}) gave a maximum impurity content of 100 parts/10^6 when the above test gases were used. Some runs were made with hydrogen of 99·9995 % purity and the figure was then 30 parts/10^6. The tube was cleaned and dried after each shock.

For the purposes of sodium-line reversal measurements (described below) a small amount of sodium chloride smoke was introduced into the test gas by passing this

over a layer of fused salt contained in a quartz tube heated to about 750 °C by a surrounding electrical furnace. The flow of test gas over the salt was controlled by a needle valve. Flame photometry of a sample of the gas from the shock tube showed that this method provided a uniform and remarkably reproducible small amount ($\sim$ 0·01 %, vol.) of sodium chloride smoke in the test gas. This smoke decomposed in less than a microsecond to give free sodium atoms behind the shock front.

Temperature measurement

The spectrum-line reversal method was used to measure the temperature history of the dissociating gases behind the shock front. The principles of this method have been described by Gaydon & Hurle (1963).

This particular adaptation of the line reversal system is shown in figure 1. It is a coaxial double-beam system able to measure temperatures to within ± 2 % in the range 1500 to 7000 °K, with a time resolution of 1 μs. It uses an Osram XBO–900 xenon arc and a tungsten Pointolite as the respective light sources for high and low temperature reversal.

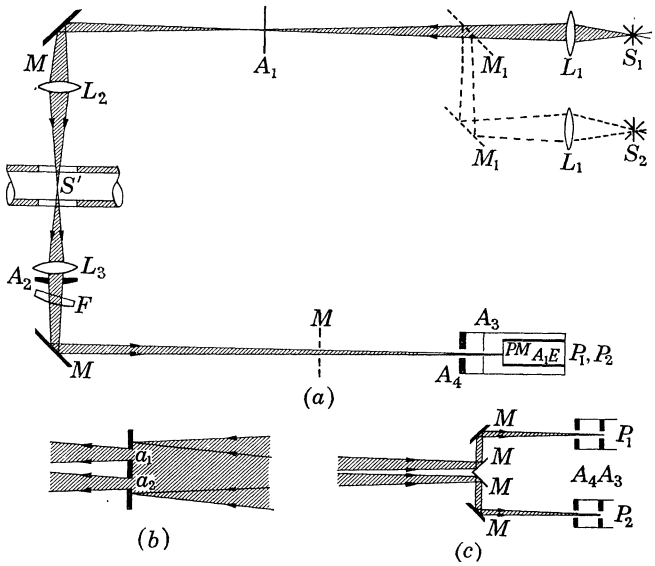

FIGURE 1. Optical arrangement of spectrum-line reversal system. (*a*) A plan view; (*b*) an enlarged elevation of the apertures used to produce the two beams; (*c*) an elevation of the periscope system of mirrors used to finally separate the two beams.

(i) *Spectrum-line reversal system*

As shown in figure 1 (*a*), an enlarged image of either the xenon arc, S_1, or the Pointolite, S_2, is focused on to the two vertically adjacent apertures a_1 and a_2 (figure 1 (*b*)) by means of the lenses, L_1, and mirrors, M_1. These illuminated apertures

constitute the two continuum sources for double-beam reversal. Their small size (1 mm diameter) and small separation (2 mm) enable reduced images of both to be focused into the centre of the shock tube at S' by the single lens, L_2. In turn, these two images are refocused onto limiting apertures covering the separate photomultipliers, P_1 and P_2, by means of the single lens, L_3, and the periscopic system of mirrors, M (figure 1 (c)). These final images are greatly magnified ones.

A single narrow-band interference filter F placed over lens L_3 serves to isolate the spectrum lines employed. The use of a single filter common to both beams eliminates any possible temperature errors that may arise owing to wavelength mismatch when separate filters are used. The filter for sodium reversal is central at 589·3 nm and has a pass band of 0·7 nm. The filter, made by Baird Atomic Ltd., has a flat-topped pass band. A monochromator is used to tune the filter *in situ*, the upper part of the slit being illuminated with the transmitted continuum and the lower part with a reference spectrum of the appropriate resonance radiation.

A single limiting aperture A_2 also placed over lens L_3 serves to ensure that each photomultiplier receives light in the same solid angle from the illuminated sources and the shocked gases. This aperture, and those (A_3, A_4) over the photomultipliers, define the spatial resolution of the light beams in the shock tube. These are approximately opposing cones having a maximum diameter of 1 mm at the windows. Owing to the coaxial optics both beams effectively traverse a common volume of gas. These optics afford 0·5 μs time resolution for the shock speeds used in this work.

The photomultipliers are a matched pair of EMI 9698. They are run at a high current ($\sim$ 5 mA) in the dynode chain to assure linearity of response at the high light intensities used. This linearity was checked with neutral filters. The outputs of the tubes are taken through a preamplifier/cathode follower circuit to the two beams of a Tektronix 502 A oscilloscope. The response time of each electronic recording system is 0·5 μs.

To measure the effective brightness temperatures of the two source apertures as imaged in the shock tube for the Pointolite source at the sodium wavelength, an optical pyrometer was used in the method described by Gaydon & Hurle (1963). For this source the temperatures of the two beams were the same. The corresponding temperatures for the xenon arc were measured as described by Hurle (1964). By varying the arc current from 20 to 50 A it is possible reproducibly to vary these temperatures from 3000 to 4250 °K. With the double-beam reversal system, it is possible to measure shock temperatures up to 7000 °K by using the source temperature of 4250 °K, both beams then being recorded in emission.

(ii) *Recording of shock temperature*

To measure shock temperatures the upper aperture a_1 (figure 1 (b)) is covered so that the photomultiplier P_1 directly records the intensity of sodium resonance emission from the hot gases. The lower photomultiplier P_2 views this line radiation against the background continuum from the source a_2. Relative to the steady level of continuum intensity, P_2 records an increase or decrease in total light intensity as

the shock passes depending on whether the resonance lines are in emission or absorption against the background; that is, if the sodium excitation temperature in the hot gases is higher or lower than the effective brightness temperature of the continuum.

The output of P_1 is displayed on the upper beam of the oscilloscope and that of P_2 on the lower. If a is the emission amplitude of the upper beam signal and b is that of the lower ($b < 0$ for absorption) then, because the two recording systems are balanced at equal sensitivity beforehand and the concentration of metal atoms in each beam is the same, the sodium excitation temperature, T^*, can be obtained at any point in the shock wave from the relation

$$\exp(-c_2/\lambda T^*) = \exp(-c_2/\lambda T_B)/(1-R),$$

where c_2 is the second radiation constant ($= 1{\cdot}438\,\mathrm{cm\,degK}$), λ is the resonant wavelength, T_B is the brightness temperature of the source image at that wavelength, and R is the ratio b/a.

The two recording systems were balanced before each shock by equating the amplitudes of the two oscilloscope signals produced by chopped modulation of the Pointolite source, both apertures being uncovered. The equivalence of this balance condition with that for resonance radiation was checked by the observation of identical oscilloscope signals under the conditions of an actual shock wave.

Interpretation of measured temperatures

A typical sodium line-reversal recording obtained for a shock wave in a 60/40 hydrogen/argon mixture is shown in figure 2 (a), and the portion immediately behind the shock front is shown expanded in figure 2 (b). Sodium emission is measured upwards. The temperature analysis of figure 2 (b) is shown in figure 3.

In the interpretation of these records and their temperature analyses, the spectrum-line reversal method measures the effective electronic excitation temperature, T^*, of the sodium atoms. These atoms are excited by collisions with the gas molecules and quenched by both collisions and radiative emission. Excitation by photon absorption is negligible at the sodium densities used. For excitation collisions with species having a Boltzmannian energy distribution at a temperature T, it can be shown that

$$\frac{[\mathrm{Na}^*]}{[\mathrm{Na}]} = \frac{g^*}{g}\exp(-c_2/\lambda T^*) = \frac{g^*}{g}\exp(-c_2/\lambda T)/(1+1/Z\tau),$$

where $[\mathrm{Na}^*]$ and g^* are the population and degeneracy of the excited state, $[\mathrm{Na}]$ and g those of the ground state, τ is the radiative lifetime of the excited state and Z is the collisional quenching frequency. Recent work by Jenkins (1966) has shown that the collisional quenching cross-section of excited sodium by hydrogen is sufficiently large ($2{\cdot}87 \times 10^{-16}\,\mathrm{cm}^2$) and independent of temperature to make the product $Z\tau$ always much greater than unity for the conditions used in the present work, so that,

effectively, $T^* \equiv T$. Furthermore, the equilibrium between these two temperatures is obtained in a time of order 10^{-8} s, so that the sodium temperature faithfully follows any changes occurring (through relaxation) in the effective temperature of the molecular degree of freedom responsible for excitation (Hurle 1964).

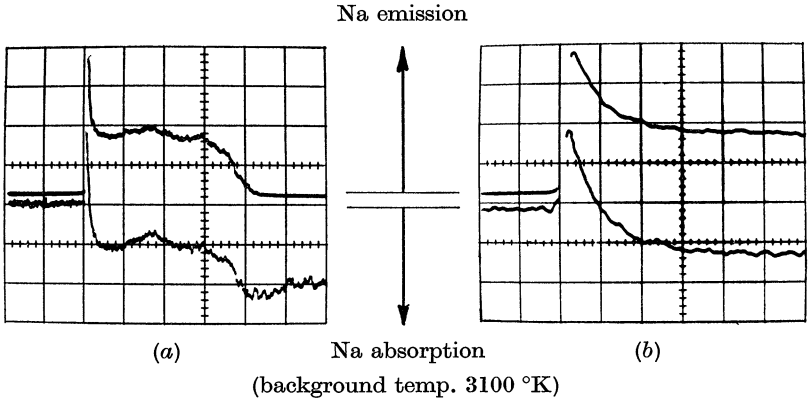

FIGURE 2. Typical sodium-line reversal records obtained from shock in 60/40:H_2/Ar mixture, showing high emission (temperature) at front followed by uniform fall to steady value as dissociation proceeds to equilibrium. Oscilloscope sweep-rate = 50 μs cm^{-1} in (*a*) and 5 μs cm^{-1} in (*b*). Wave speed = 3·34 mm μs^{-1}: initial pressure = 13·2 Torr. T_0 (obs.) = 3560 °K T_0 (calc.) = 3550 °K; T_e (obs.) = 2910 °K T_e (calc.) = 2925 °K. Shock pressure (obs.) = 1·12 atm; (calc.) = 1·13 atm. Degree of dissociation (α_e) = 6·89 × 10^{-2}.

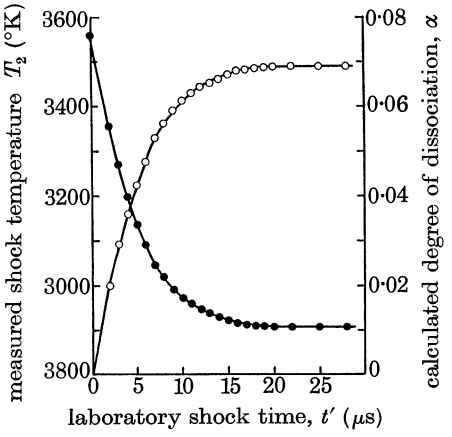

FIGURE 3. Measured temperature profile for the record shown and described in figure 2. The degree of dissociation, α, calculated as in appendix I, is also shown (open circles).

The particular degree of freedom has been shown in many cases (see, for example, Gaydon & Hurle 1963; Hurle 1964) to be the vibrational one. Observations (Gaydon & Hurle 1961, 1962) with sodium- and chromium-line reversal in hydrogen/argon shock waves have revealed a lag in excitation at the shock front which was attributed

to the hydrogen vibrational relaxation process, and this has since been confirmed in more extensive relaxation studies by Kieffer & Lutz (1967) using a laser–schlieren system.

The work of Kieffer & Lutz shows that the vibrational relaxation time of hydrogen is extremely short, decreasing from 6×10^{-7} to 2×10^{-7} s atm ($6{\cdot}08 \times 10^{-2}$ to $2{\cdot}03 \times 10^{-2}$ s N m^{-2}) between 2500 and 4000 °K. In the present work, the hydrogen dissocation-relaxation times are correspondingly much longer than this. Typically, at 2500 °K a hydrogen molecule undergoes about $1{\cdot}5 \times 10^5$ collisions s^{-1} that result in vibrational excitation while only 10^3 lead to dissociation; at 4500 °K the corresponding collision numbers are 10^6 and 2×10^4 s^{-1}. Thus, the vibrational degree of freedom can be expected to remain Boltzmannian and in equilibrium with the kinetic temperature of the gas during the dissociation process. There are, therefore, good reasons to believe that the sodium excitation temperature, or measured line-reversal temperature, is the same as the gas kinetic temperature in the present experiments.

With this interpretation of the measured temperatures the records shown in figure 2 and their analysis in figure 3 can be discussed further. In these, the gas temperature rises to a high value at the shock front (at a rate determined only by the resolution of the recording system), and then decreases smoothly to an equilibrium value as the enthalpy of the gas falls owing to molecular dissociation. The 'frozen' temperature observed at the shock front (figure 3) agrees well with that calculated (appendix II) from the wave speed for full vibrational equilibrium but no dissociation, while the temperature observed at equilibrium also agrees with that calculated for full thermodynamic equilibrium. Such correspondences were observed for all the shock waves studied in the present work.

The rate of temperature fall in figure 3 is a measure of the rate of dissociation. Chemical rate constants were evaluated from such temperature profiles by the methods described in the next section. It is noted in this respect that, because the intensity of optical emission is strongly dependent on temperature (varying at 589·3 nm as T^{10} at 2500 °K and T^5 at 5000 °K) and also because the temperature fall owing to even a small amount of dissociation is large, the spectrum-line reversal method affords an extremely sensitive monitor of the progression of the dissociation process. It is also noted that, as illustrated by figures 2 and 3, the region of dissociation occupies only a small portion of the total hot gas flow, so that wave attenuation (which was observed always to be small, as the constancy of the equilibrium emission and temperature indicates) and other boundary-layer effects did not influence the temperature profiles.

Chromium-line reversal

At various stages during the course of these experiments, observations were made in which chromium was used in place of sodium as the reversal element. For this purpose, the sodium chloride was replaced by 0·1 % (vol.) of the volatile chromium

carbonyl. In both cases the observed temperature profiles were identical for similar shock conditions.

These results serve to confirm the following points: (1) The measured excitation temperatures are equal to the gas kinetic temperatures. (2) The presence of the small amount of metal atom compound does not influence the dissociation process.

3. Evaluation of rate constants

The studies of hydrogen dissociation covered a range of frozen shock temperatures from 2750 to 7000 °K with corresponding equilibrium temperatures running from 2560 to 4100 °K. The shock pressures ranged from 0·6 to 1·8 atm (60·8 to 182·4 kN m^{-2}).

These studies provide, for each shock, a number of points at which the temperature and the time after passage of the shock front are known. We have reduced these data by two essentially different methods which can be called analytic and synthetic.

In both analyses it is assumed that six reactions take place behind the shock, namely

$$H_2 + M_i \underset{k_{-i}}{\overset{k_i}{\rightleftharpoons}} H + H + M_i \quad (i = 1, 2, 3). \tag{1}$$

The third body M_i is H_2, H or Ar for $i = 1$, 2 or 3. It is further assumed that the forward and reverse rate constants k_i and k_{-i} are at all times related to the molar equilibrium constant K_c by the equation

$$\frac{k_i}{k_{-i}} = K_c = \frac{[H]^2}{[H_2]}. \tag{2}$$

The validity of this assumption, even well away from equilibrium at the beginning of the shock, is borne out by the results (see the discussion in the next section).

The analytic reduction

In the analytic method the temperature is expressed as an analytic function of the time, and the rate constants for the reactions involved are obtained at a number of arbitrary temperatures for each shock. No specific functional temperature-dependence is assumed for the rate constants. On the other hand, the success of the method depends on the choice of analytic functions to represent the temperature-time profiles. The detailed mathematical treatment is to be found in appendix I. Essentially it yields, as a function of temperature, a parameter, γ, which is a linear combination of the three recombination rate constants

$$\gamma(T) = (2k_{-2} - k_{-1})\,\alpha + k_{-1} + \{(1-\beta)/\beta\}\,k_{-3}. \tag{3}$$

In this expression β is the mole fraction of hydrogen in the initial hydrogen–argon mixture and α is the degree of dissociation, varying with temperature from zero at T_0 to its equilibrium value α_e at T_e.

As is shown in appendix I, $\gamma(T)$ is obtained as the product of two factors,

$$\gamma(T) = F(T)\,\mathrm{d}T/\mathrm{d}t'.$$

$F(T)$ is a complicated function whose value is, however, exactly calculable at any temperature between T_0 and T_e. We obtain $\mathrm{d}T/\mathrm{d}t'$, the derivative of the temperature with respect to laboratory time t', from the experimental plots of temperature against laboratory time, in the following manner. Since γ remains finite for all values of T including T_e, it follows, from equation (A 2) in appendix I that $\mathrm{d}T/\mathrm{d}t'$ approaches zero linearly with T as $T \to T_e$. We therefore considered the general family of curves

$$\frac{\mathrm{d}T}{\mathrm{d}t'} = -a_1(T - T_e^*)\left[1 + b\frac{T_0 - T}{T_0 - T_e^*}\right], \tag{4}$$

with the boundary conditions

$$T \to T_e^* \quad \text{as} \quad t' \to \infty, \qquad T \to T_0 \quad \text{as} \quad t' \to -a_0/a_1.$$

T_e^* was arbitrarily chosen to be very slightly less than the measured T_e, to allow for the fact that $t'(T_e)$ is finite. The difference $T_e - T_e^*$ was never greater than a fraction of a degree and has no physical significance. It was introduced only for mathematical convenience, to improve the fit with the experimental data. The second boundary condition contains the parameter a_0, to allow for the small ($< 0{\cdot}1\ \mu$s) experimental uncertainty in the origin of the time axis.

When $b = 0$, equation (4) is equivalent to the exponential fit, whereas $b = 1$ corresponds to a tanh function. Intermediate values of b generate more or less concave curves for T as a function of t'. For a given value of b, the values of a_0 and a_1 were obtained by a least squares fit of the experimental points. The deviation was then minimized by varying b. Optimum values of b ranged from $2{\cdot}0$ to $-0{\cdot}9$. In all cases the ratio a_0/a_1 was well within the experimental uncertainty of the time origin, and in nearly every case, the standard error was less than 10 °K.

From a knowledge of $\gamma(T)$ at all temperatures between T_0 and T_e for each shock, it is a relatively easy matter to obtain the individual rate constants as functions of temperature.

The synthetic reduction

In the synthetic method the form for the recombination rate constants is assumed to be

$$k_{-i} = A_{-i}/T^{n_{-i}}.$$

Guesses are made at the values of the six parameters, A_{-1}, A_{-2}, A_{-3}, n_{-1}, n_{-2}, n_{-3} and the temperature–time profile is synthesized by numerical integration of the differential and kinetic shock equations. From the comparison of this profile with the experimental results new and improved guesses for the parameters are computed and the above procedure repeated until the best possible agreement, in the least squares sense, has been obtained.

The significant feature of this method lies in the optimization of the convergence procedure and is based on the ideas of Marquardt (1963, 1966). The method, which is applicable to the solution of many 'best-fit' problems when the equations are non-linear in the parameters to be estimated, is described in appendix IV.

In essence, the technique combines the best features of two well-known methods for solving non-linear estimation problems, the 'steepest descent' method and the 'Taylor series' method. The steepest descent method ensures that an improvement in the fit is obtained at each iteration but converges very slowly, while the 'Taylor series' method does not necessarily give an improvement in the fit each iteration but converges very rapidly as soon as the parameter values are close to the optimum. At the start of the procedure a large element of 'steepest descent' is used to ensure a rapid improvement in the parameter values and as the calculation proceeds more and more of the 'Taylor series' element is included to speed up the convergence.

Both of these techniques require values of the derivatives of the calculated solution with respect to each of the unknown parameters. This means that in the present work the differential equations must be solved at least seven times at each iteration. Thus it is clear that unless convergence can be obtained in a small number of iterations this technique will be very time-consuming, in contrast to the analytic method. Because of this, and because this technique was used partly as a check on the validity of the first method, we decided not to proceed with those experimental runs which did not converge in a reasonable number of iterations.

It is particularly satisfying that the results obtained by the two methods are in close agreement.

4. Results and discussion

k_{-1} *and* k_{-3} (H_2 *and* Ar *as third bodies*)

The result of the analytic reduction of the data is a knowledge of $\gamma(T)$ (equation (3)), from which it is evident that at T_0, where no dissociation has yet taken place,

$$\gamma(T_0) = k_{-1}(T_0) + \frac{1-\beta}{\beta} k_{-3}(T_0), \tag{5}$$

so that each shock yields one point for these two rate constants. Separation of k_{-1} and k_{-3} was achieved by a combination of variation and least squares fitting, to obtain the minimum deviation. Results (shown in figures 4 and 5) are

$$\log_{10} k_{-1} = 15{\cdot}243 - 1{\cdot}95 \times 10^{-4} T \text{ cm}^6 \text{ mole}^{-2} \text{ s}^{-1},$$
$$\log_{10} k_{-3} = 15{\cdot}787 - 2{\cdot}75 \times 10^{-4} T \text{ cm}^6 \text{ mole}^{-2} \text{ s}^{-1},$$

with a standard deviation of 0·193 in $\log_{10} k_{-1}$. These temperature dependencies are equivalent to about T^{-2} around 3000 °K. Some of the scatter may be due to the experimental range of temperature (over which the fitting was optimized) falling far short of T_0 for some of the high-temperature shocks, because of the finite-time resolution of the experimental method. In these cases the best fit would not therefore necessarily yield the best estimate of $\mathrm{d}T/\mathrm{d}t'$ at T_0.

The ratio k_{-3}/k_{-1} equals 1·8 at 3600 °K and decreases to unity at 6800 °K. This variation is probably not significant, since the line obtained by assuming $k_{-1} = k_{-3}$, i.e.

$$\log_{10} k_{-1} = \log_{10} k_{-3} = 15{\cdot}542 - 2{\cdot}37 \times 10^{-4} T \text{ cm}^6 \text{ mole}^{-2} \text{ s}^{-1}$$

has a standard deviation of 0·195, practically the same as for the 'optimum' fit.

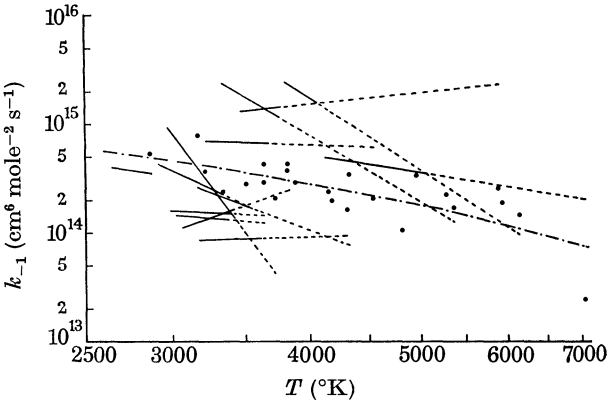

FIGURE 4. k_{-1} (H + H + H_2) as a function of temperature. ——, - - - -, synthetic reduction (solid line indicates experimental range of temperatures fitted); ●, analytic reduction; –·–·, optimum fit, analytic reduction.

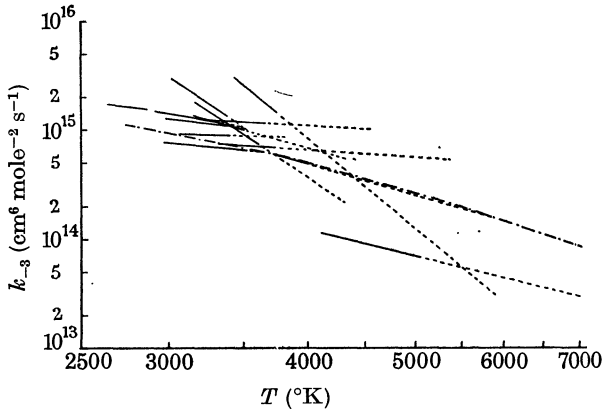

FIGURE 5. k_{-3} (H + H + Ar) as a function of temperature. ——, - - - -, synthetic reduction (solid line indicates range of temperatures used in fitting process); –·–·–, optimum fit, analytic reduction.

The results obtained by the synthetic reduction are summarized in table 1. For each experimental run the least squares estimates of the six parameters (A_{-i}, n_{-i}; $i = 1, 2, 3$) are given together with the mole fraction of hydrogen in the test gas, the calculated frozen and equilibrium temperatures, the range of the temperature used in the fitting process and the degree of dissociation and the pressure in the

PROCEEDINGS OF THE ROYAL SOCIETY A MATHEMATICAL, PHYSICAL & ENGINEERING SCIENCES
PROCEEDINGS OF THE ROYAL SOCIETY A MATHEMATICAL, PHYSICAL & ENGINEERING SCIENCES

Table 1. Results of the synthetic reduction

run no.	β	temperature range (°K): T_0	temperature range (°K): highest temperature in fitting process	T_e	P_e (atm)	α_e	$\log_{10} A_{-1}$	n_{-1}	$\log_{10} A_{-2}$	n_{-2}	$\log_{10} A_{-3}$	n_{-3}	Δt (s)	standard error (°K)
33	0·6	2866	2851	2647	1·325	0·0257	19·77	1·51	21·54	1·62	20·36	1·50	$0{\cdot}3 \times 10^{-7}$	3·2
46	0·6	3213	3215	2798	1·123	0·0488	34·34	5·61	23·26	2·05	21·86	1·88	$-0{\cdot}3 \times 10^{-5}$	6·4
54	0·6	3491	3325	2904	1·132	0·0693	31·43	4·85	14·60	−0·44	21·65	1·87	$-0{\cdot}9 \times 10^{-6}$	3·5
59	0·5	4398	3601	3166	1·252	0·1538	12·95	−0·28	15·27	−0·08	39·15	6·83	$0{\cdot}3 \times 10^{-7}$	5·8
61	0·5	4316	3518	3150	1·078	0·1583	27·81	3·83	12·33	−0·94	25·06	2·84	$0{\cdot}5 \times 10^{-7}$	6·8
63	0·5	5359	3740	3317	0·756	0·2798	36·78	6·08	17·21	0·56	17·27	0·68	$-0{\cdot}3 \times 10^{-6}$	7·4
67	0·5	3615	3358	3006	1·809	0·0823	17·18	0·87	18·64	0·91	39·86	7·01	$-0{\cdot}1 \times 10^{-6}$	9·3
68	0·5	3805	3391	3055	1·579	0·1016	0·56	−3·87	21·60	1·66	15·76	0·23	$0{\cdot}6 \times 10^{-7}$	8·5
70	0·4	4543	3660	3230	1·098	0·2116	16·14	0·37	15·55	−0·0025	16·98	0·54	$-0{\cdot}1 \times 10^{-5}$	5·6
71	0·4	5872	3751	3444	0·753	0·3944	11·23	−1·10	12·60	−0·61	45·14	8·39	$0{\cdot}1 \times 10^{-6}$	8·0
72	0·4	3620	3396	2984	1·252	0·1022	15·83	0·47	24·33	2·43	19·80	1·35	$0{\cdot}2 \times 10^{-7}$	3·0
78	0·2	7033	5052	4110	1·202	0·8408	20·66	1·65	50·83	9·67	23·31	2·56	$0{\cdot}2 \times 10^{-7}$	18·4
81	0·2	6141	4030	3780	1·113	0·6782	39·25	6·67	35·52	5·50	25·27	2·94	$-0{\cdot}7 \times 10^{-9}$	8·9
92	0·6	3704	3510	2952	0·927	0·0889	63·59	14·00	8·91	−1·99	18·46	1·03	$-0{\cdot}6 \times 10^{-6}$	19·2

equilibrium gas. As was mentioned earlier, there was some doubt about the exact zero on the time scale of the traces and so a quantity Δt was added to all the experimental times and included as a seventh parameter to be estimated. The least squares estimates of Δt are also included in the table. In order to give an idea of the agreement between the predicted and experimental temperatures within one run we have included an estimate of the standard error of the fit.

These results are also shown in figures 4 and 5, for comparison with those given by the analytic method. Each line represents the rate constant for a particular shock, from T_0 to T_e, the solid part of the line showing the temperature range used in the fitting process. It is seen that the over-all agreement between the two methods of analysis is very satisfactory.

Comparison with other results

The analytic results are compared with other recent evaluations in figures 6 and 7. In all the shock tube experiments, a combination of k_{-1} and k_{-3} is measured and, as here, the separation is achieved by studying the effects of changing mixture composition. The main disagreement with previous work lies in the values obtained for the ratio k_{-3}/k_{-1}. Whereas we obtain a value $\geqslant 1$, others have found values lying between 0·1 and 0·5. By neglecting k_{-3} in equation (5) we may obtain an upper bound for k_{-1},

$$\log k_{-1}\ (\text{upper bound}) = 15{\cdot}505 - 1{\cdot}37 \times 10^{-4} T\ \text{cm}^6\,\text{mole}^{-2}\,\text{s}^{-1}$$

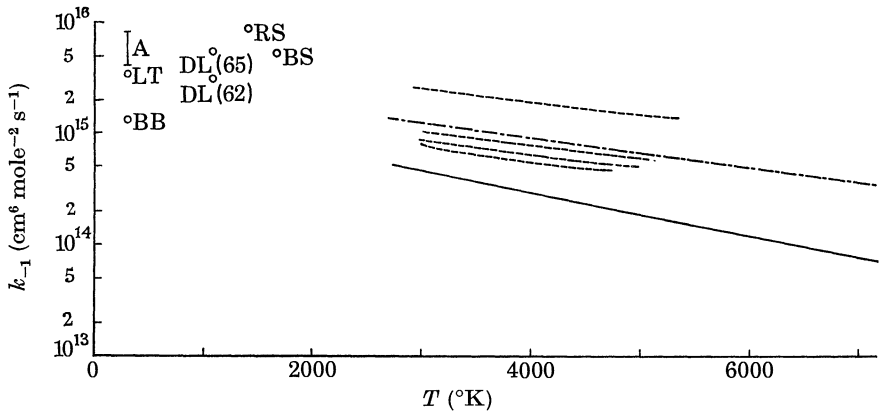

FIGURE 6. k_{-1} as a function of temperature; comparison with other work. Room temperature: A, Amdur (1935, 1938), Amdur & Robinson (1933); BB, Bennett & Blackmore (1968); LT, Larkin & Thrush (1964, 1965). Flames: BS, Bulewicz & Sugden (1958); DL, Dixon-Lewis, Sutton & Williams (1962, 1965); RS, Rosenfeld & Sugden (1964). Shock tubes: J, Jacobs, Geidt & Cohen (1967); P, Patch (1962); R, Rink (1962); S, Sutton (1962); ——, present work, optimum fit; –·–·–, present work upper bound, assuming $k_{-3} = 0$.

with a standard deviation of 0·26 in $\log_{10} k_{-1}$. In so far as one may interpret results of other workers for k_{-1} as being equivalent to an upper bound (k_{-3} essentially neglected), it is seen from figure 6 that agreement is excellent. Extrapolation to

lower temperatures also shows excellent agreement with the most reliable room-temperature work though the results from flames for k_{-1} are higher than might be expected by extrapolation of our line.

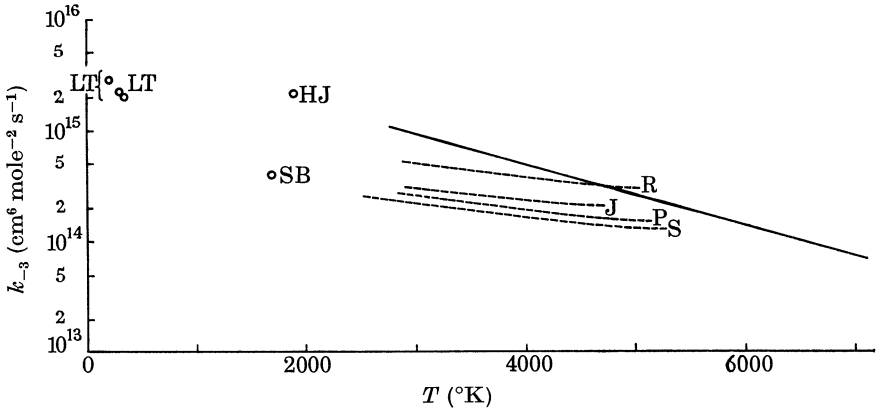

FIGURE 7. k_{-3} as a function of temperature; comparison with other work. Room temperature: LT, Larkin & Thrush (1964, 1965). Flames: HJ, Halstead & Jenkins (1968). Shock tube: SB, Schott & Bird (1964); J, Jacobs, Geidt & Cohen (1967); P, Patch (1962); R, Rink (1962); S, Sutton (1962); ——, present work, optimum fit.

k_{-2}(H *as third body*)

Having obtained the temperature-dependences of k_{-1} and k_{-3} we can substitute these back into $\gamma(T)$, equation (3), to obtain k_{-2} at all temperatures between T_0 and T_e. We thus obtain for k_{-2} (as a function of temperature) a line for each shock, rather than a point. The results are shown in figure 8. The extreme envelopes and the mean line through these results are compared with the results of the synthetic method in figure 9 and with other results in figure 10. Because the equilibrium dissociation of H_2 decreases rapidly with temperature, it is not surprising that the scatter should be largest at the lower end of the temperature range. Despite the relatively large scatter, however, three important conclusions may be drawn from figure 8.

The first point relates to our assumption in equation (2) that the law of mass action is valid at all points along the shock, from T_0 (far from equilibrium) to T_e (at equilibrium). It will be seen from figure 8 that a given temperature, 4200 °K, for example, corresponds in different shocks to different relative positions away from equilibrium. Yet within experimental error, the same value for the rate constant is obtained (certainly there are no consistent trends within the scatter). It may therefore be said that equation (2) is validated by the self-consistent results of our treatment. Furthermore, the value of k_{-i} is independent of the degree of equilibration.

The two other conclusions are that there is a steep temperature-dependence (T^{-6}) at temperatures in excess of 4000 °K and a very marked reduction in slope at lower temperatures with a strong indication of a maximum value of k_{-2} around 3000 °K.

We are confident (because of internal checks) that the marked changes in slope

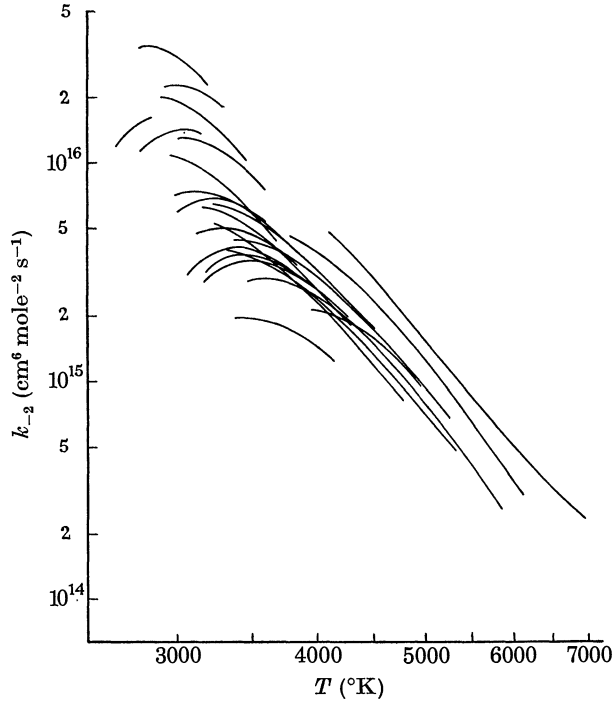

FIGURE 8. k_{-2} (H+H+H) as a function of temperature: analytic reduction. Each line represents the results from T_0 to T_e for a single shock.

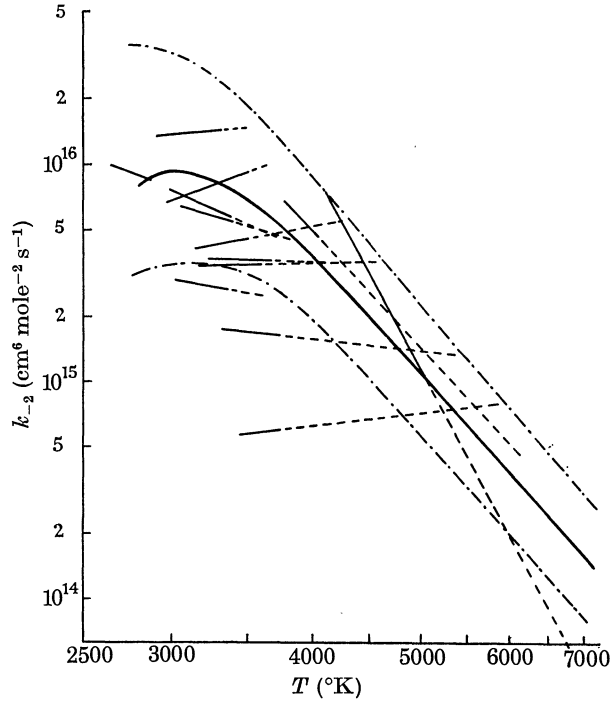

FIGURE 9. k_{-2} as a function of temperature: synthetic reduction. Also shown are the mean line (—) and extreme envelopes (–·–·–·) of the analytical results.

for any individual shock are not due to our mathematical methods, but represent a real phenomenon. They are certainly not due to an inaccurate repartition of $\gamma(T)$ among k_{-2}, k_{-1} and k_{-3}. In many runs $\gamma(T)$ itself exhibited a maximum as a function of temperature (and in one case decreased with decreasing temperature from T_0 to T_e). The synthetic method of analysis also supports these conclusions, as can be seen from figure 9.

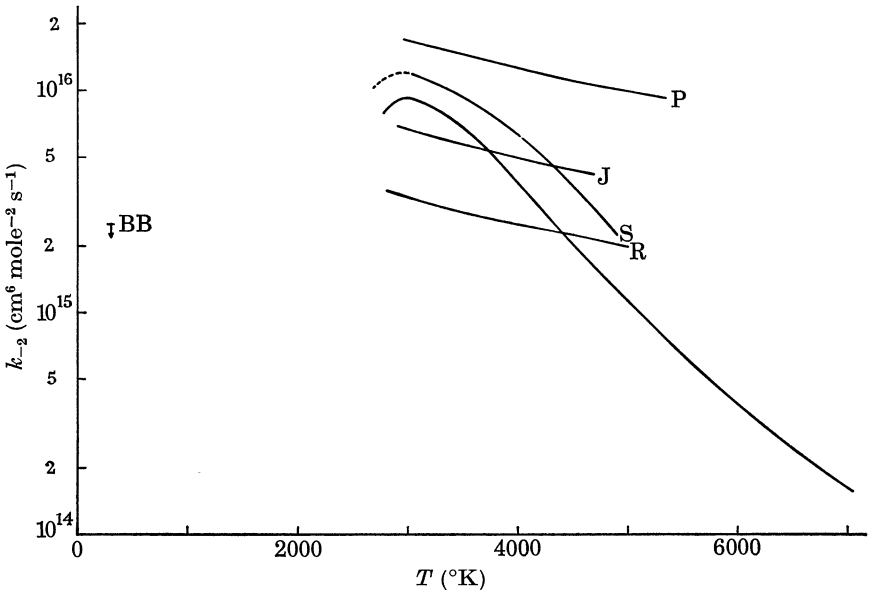

FIGURE 10. k_{-2} as a function of temperature; comparison with other work. BB, upper limit at room temperature, Bennett & Blackmore (1968); J, Jacobs, Geidt & Cohen (1967); P, Patch (1962); R, Rink (1962); S, Sutton (1962); ——, present work.

When our results are compared with those of others, the following cautionary remarks are in order. Patch (1962), Rink (1962), and Jacobs, Giedt & Cohen (1967) all assume a temperature-dependence of T^{-1}, and their results can therefore only be used as confirmation of the order of magnitude of the rate constant at these temperatures. It is significant that neither Patch nor Rink consider their data to be sufficient to determine the temperature-dependence. Indeed Patch states: 'the best match was obtained for T^{-1}, but its superiority over T^{-4} depended solely on experiment no. 17'. Similarly, Rink: '. . . the value of T^{-3} with appropriate changes in the constant to retain the same rate at 3000 °K was found to produce no significant changes. . .', Jacobs *et al.* do not make any comment on this point. We have not included the earlier work of Gardiner & Kistiakowsky (1961), because, although their values for k_{-2} agree with those here quoted, their results are, in our opinion, invalidated by the improbably low values for k_{-1} obtained in the same experiments.

The excellent agreement with Sutton's work (1962) is particularly pleasing. In his paper Sutton does not indicate a maximum in the rate constant at 3000 °K, although

a close examination of his figure 8 reveals very strong indications of a maximum at that point. We have drawn as a dotted line in figure 10 the extension (through his own data) of the line Sutton published. We consider this to be important independent confirmation of the physical reality of the maximum in k_{-2} at about 3000 °K.

Further evidence that such a maximum exists comes from an examination of the scanty results at room temperature. The most recent estimate is that of Bennett & Blackmore (1968) who give an *upper limit* for k_{-2} of $2{\cdot}5 \times 10^{15}$ cm^6 mole^{-2} s^{-1} at 300 °K. Similarly, the most carefully analysed prewar data (Amdur & Robinson 1933; Amdur 1935, 1938) suggest a range of values of $5\text{–}10 \times 10^{15}$ cm^6 mole^{-2} s^{-1} at room temperature, which values must again be regarded as an upper limit, since the presence of water (and, in some of the work, of the wall reactions) was neglected in the analysis, and water is known to accelerate the hydrogen atom recombination in discharge systems (Larkin & Thrush 1965). There seems little doubt therefore that k_{-2} is substantially lower at 300 °K than at 3000 °K and exhibits a maximum as a function of temperature.

Proposed mechanism for the three-atom process

When k_{-2} is compared with k_{-1}, it is seen that k_{-2} is much greater at 3000 °K, but that its upper limit at 300 °K is about equal to the value of k_{-1} at that temperature. The two rate constants also appear to approach each other in magnitude at temperatures greater than 7000 °K.

Considering the third body as an inert energy sink, one would expect a hydrogen atom to be about as efficient as Ar or H_2 in stabilizing an orbiting pair of hydrogen atoms through inelastic (non-reactive) collisions.* All these factors, when taken together, suggest the existence of a 'resonance' in the three-atom rate constant, k_{-2}, due to some mechanism other than straightforward collisional stabilization. The initial increase with temperature of k_{-2} implies that such a mechanism requires an activation energy, whilst its subsequent decrease suggests that the products become unstable at higher temperatures. We have proposed that the atom exchange reaction is a probable candidate. The details of a simple classical calculation have been published elsewhere (Hurle, Mackey & Rosenfeld 1968) and we limit ourselves here with a brief description to demonstrate the plausibility of the suggestion.

An atom-exchange process requires an activation energy, E_a (classically equal to the energy barrier along the reaction coordinate), at least when the molecule is in a low vibrational state. If the vibrational mode is assumed to be adiabatic during the time scale of the exchange process (about 10^{-14} s), one may expect E_a to be independent of the degree of vibrational excitation. We assume the two-step process:

$$\mathrm{H}(1) + \mathrm{H}(2) \rightleftharpoons \mathrm{H}_2^{v,J}(1,2)$$

$$\mathrm{H}_2^{v,J}(1,2) + \mathrm{H}(3) \rightarrow \mathrm{H}_2^{v,J'}(1,3) + \mathrm{H}(2).$$

* *Note added in proof*. A very relevant discussion of this normal stabilization is presented by Roberts, R. E., Beinstein, R. B. & Curtiss, C. F. 1968 *Chem. Phys. Lett.* **2**, 366.

Here v and J are the vibrational and rotational quantum numbers respectively. Our assumption of vibrational adiabaticity means that v is conserved. The product molecule will only be stable if J' is less than some critical value, which in turn implies a limit on the relative kinetic energy of approach of H(1) and H(2) for successful stabilization.

Hurle *et al.* (1968) considered a simple model based on this idea. They estimated the equilibrium constant for the first process (including the effect of the rotational barrier). Using reasonable estimates for the energy barrier and collision diameter associated with the second step, and averaging properly over the Maxwellian distribution of the relative velocities, they obtained a recombination rate constant whose value at 3000 °K was about 10^{16} cm^6 mole^{-2} s^{-1}, and which, as a function of temperature, exhibited a maximum around 2000–2500 °K. The decrease with increasing temperature was however much too slow, which suggests that their simple classical model overestimates the number of stabilizing collisions at the higher temperatures. The agreement is sufficiently good to be encouraging and we are proceeding with a more detailed calculation to test our assumptions, particularly that of vibrational adiabaticity.

The authors are indebted to W. J. Gressler for help in the design of the shock tube; to P. J. Swain for most enthusiastic assistance with the experiments; and to members of the Mathematics Division for help with the computations.

Appendix I. Derivation of $\gamma(T)$ for the analytic reduction

If the concentrations in mole cm^{-3} are represented by square brackets, the total rate of change of hydrogen-atom concentration at any time, t (in shock-fixed coordinates), behind the shock is

$$\frac{\mathrm{d}[\mathrm{H}]}{\mathrm{d}t} = \left(\frac{\partial[\mathrm{H}]}{\partial t}\right)_\rho + \left(\frac{\partial[\mathrm{H}]}{\partial \rho}\right)_t \frac{\mathrm{d}\rho}{\mathrm{d}t},$$

where the first derivative is the real change due to dissociation and the other term is that due to the changing gas density, ρ. This term can be eliminated by working in terms of the degree of dissociation, α. Thus, for a given value of β, the relevant concentrations at any subsequent times during the dissociation process are

$$[\mathrm{H}_2] = \beta(1-\alpha)\rho/M_1, \quad [\mathrm{H}] = 2\alpha\beta\rho/M_1[\mathrm{Ar}] = (1-\beta)\rho/M_1,$$

where ρ is the local density of the shocked gas and M_1 is its initial molecular weight. (Throughout these appendices the subscripts 1, 0 and e refer to the initial unshocked gas, the frozen shocked gas and the equilibrium shocked gas respectively. The conventional use of the subscript 1 for the initial unshocked gas should not lead to confusion despite the simultaneous use of the same subscript for one of the rate constants).

From the reaction mechanism, equation (1), we obtain the local chemical rate of change of the hydrogen-atom concentration,

$$\left(\frac{\delta[\mathrm{H}]}{\mathrm{d}t}\right)_\rho = 2k_1[\mathrm{H_2}]^2 + 2k_2[\mathrm{H_2}][\mathrm{H}] + 2k_3[\mathrm{H_2}][\mathrm{Ar}] - 2k_{-1}[\mathrm{H}]^2[\mathrm{H_2}] - 2k_{-2}[\mathrm{H}]^3 - 2k_{-3}[\mathrm{H}]^2[\mathrm{Ar}],$$

The equation of state may be written as

$$\rho = PM_1/[RT/1+\alpha\beta)],$$

where P and T are the local pressure and temperature respectively. A combination of these equations yields

$$\frac{\mathrm{d}\alpha}{\mathrm{d}t} = \frac{P}{(RT)^2}\frac{\beta}{1+\alpha\beta}\left[K_P(1-\alpha) - \frac{4\alpha^2\beta P}{1+\alpha\beta}\right]\left[k_{-1}(1-\alpha) + 2k_{-2}\alpha + k_{-3}\frac{1-\beta}{\beta}\right],$$

where $K_P = K_c RT$.

Another relation between α and T is obtained from a consideration of the conservation of energy along the shock. The enthalpy H (in cal g^{-1}) of the mixture at the temperature T is related to its value at equilibrium by the relation

$$H = H_e + \frac{1}{2\times 10^7 J}(u_e^2 - u^2) - \Delta E + \Delta E_e$$

where J is the Joule equivalent of heat, u is the gas velocity relative to the shock front, related to the shock speed W by

$$u = W\rho_1/\rho$$

and ΔE (cal g^{-1}) is the energy in the dissociated bonds, related to the dissociation energy E_D (cal mole^{-1}) by $\Delta E = \alpha\beta E_D/M_1$.

The total enthalpy can also be written in terms of the concentrations and the enthalpies $h_i(T)$ (cal mole^{-1}) of the species i,

$$H = [\beta(1-\alpha)h_1 + 2\alpha\beta h_2 + (1-\beta)h_3]/M_1.$$

By a manipulation of the above equations we obtain a relation between α and T of the form

$$A(T)\alpha^2 + B(T)\alpha + C(T) = 0, \qquad \text{(A 1)}$$

where

$$A = \phi\frac{T^2\beta^2}{P^2},$$

$$B = 2\phi\frac{T^2\beta}{P^2} + \beta E_D + 2\beta h_2 - \beta h_1,$$

$$C = \phi\frac{T^2}{P^2} - \phi\frac{T_e^2(1+\alpha_e\beta)^2}{P_e^2} - \alpha_e\beta E_D + h_1\beta + (1-\beta)h_3 - H_e,$$

with

$$\phi = \frac{M_1 W^2 P_1^2}{2\times 10^7 J T_1^2}.$$

The local pressure P varies from its value P_0 at the shock front to P_e at equilibrium. We have allowed for this small change ($< 5\,\%$), by assuming that P varies linearly

with T. This small correction enables us to have numerical self-consistency in our equations without significantly affecting the results (as confirmed in sample calculations with P treated as a constant, equal to its mean value). Differentiation of equation (A 1) yields $\mathrm{d}\alpha/\mathrm{d}T$.

The transformation of the time variable from the shock-fixed coordinate (t) to the laboratory co-ordinate (t') is accomplished by the relation

$$\frac{\mathrm{d}t}{\mathrm{d}t'} = \left[\frac{\rho}{\rho_1}\right]_{t'} = \left[\frac{PT_1}{P_1T(1+\alpha\beta)}\right]_{t'}.$$

This leads us to our final expression for the rate constants,

$$\gamma \equiv (2k_{-2}-k_{-1})\,\alpha + k_{-1} + \frac{1-\beta}{\beta}\,k_{-3} = \frac{\mathrm{d}T}{\mathrm{d}t'}\left\{\frac{\mathrm{d}\alpha}{\mathrm{d}T}\,\frac{R^2P_1T^3(1+\alpha\beta)^2}{P^2T_1\beta\,[K_P(1-\alpha)-4\alpha^2\beta P/(1+\alpha\beta)]}\right\}. \quad \text{(A 2)}$$

The expression in braces, referred to as $F(T)$ in the text, can be evaluated exactly at arbitrary temperatures between T_0 and T_e, the initial and equilibrium conditions being given. Values of α_e, T_0, W, P_0 and P_e are obtained by solving the shock equations, P_1, ρ_1, T_1, β and T_e being given (see appendix II).

Appendix II. The calculation of the conditions immediately behind an incident shock front given the unshocked gas conditions and the equilibrium temperature

The continuity equations in shock-fixed coordinates, the equation of state, the atom balance and the equilibrium condition may be written down in the form

$$\rho u = \text{const.},$$

$$P + \rho u^2 = \text{const.},$$

$$2\times 10^7 J\,[H+\Delta E] = u_1^2 - u^2,$$

$$PM = R\rho T,$$

$$M = \frac{M_1}{1+\alpha\beta},$$

$$K(T_e) = \frac{4\alpha_e^2\beta R T_e \rho_e}{(1-\alpha_e)\,M_1}.$$

The quantities in these equations are defined in appendix I.

If we represent the unknowns α_e, ρ_1/ρ_e, u_1, P_0, ρ_1/ρ_0, T_0 as x_1, x_2, x_3, x_4, x_5, x_6, then simple algebraic manipulation of these equations (applied at T_1, T_0 and T_e) gives six simultaneous non-linear equations which may be solved for the six unknowns $x_1, \ldots, x_6$ by the generalized Newton–Raphson iteration technique.

If we write these equations as

$$f_j(x_1, \ldots, x_6) = 0 \quad (j = 1, \ldots, 6),$$

and if $x_1^0, \ldots, x_6^0$ is an approximation to the solution, then we expand the functions f in Taylor series up to first-order terms as follows

$$f_j(x_1^1, \ldots, x_6^1) = f_j(x_1^0, \ldots, x_6^0) + \sum_{k=1}^{6} \Delta x_k \left(\frac{\partial f_j}{\partial x_k}\right) + O(\Delta x^2) \quad (j = 1, \ldots, 6),$$

where $x_k^1 = x_k^0 + \Delta x_k$, with derivatives evaluated at $x_k = x_k^0$.

If we now assume that the x_k^1 are the solutions and that all terms of higher order than the first are zero, then we have the following system of linear equations:

$$\sum_{k=1}^{6} \Delta x_k \left(\frac{\partial f_j}{\partial x_k}\right)_{x_0} = -f_j(x_1^0, \ldots, x_6^0) \quad (j = 1, \ldots, 6)$$

which may be solved for the Δx_k, which may then be used to calculate the x_k^1. Because of the assumptions made above these will not be the correct solutions and the process will have to be repeated with the x_k^0 replaced by the x_k^1.

This technique was used in both methods of analysis presented in this paper; convergence to the solution was obtained in all cases in a small number of iterations.

Appendix III. The differential equations representing the state of the gas behind a normal shock front

The basic continuity equations and the equation of state (appendix II) are differentiated with respect to laboratory time t' to give:

$$\rho \frac{\mathrm{d}u}{\mathrm{d}t'} + u \frac{\mathrm{d}\rho}{\mathrm{d}t'} = 0,$$

$$2u\rho \frac{\mathrm{d}u}{\mathrm{d}t'} + u^2 \frac{\mathrm{d}\rho}{\mathrm{d}t'} + \frac{\mathrm{d}P}{\mathrm{d}t'} = 0,$$

$$S \frac{\mathrm{d}T}{\mathrm{d}t'} + \frac{M_1 u}{J \times 10^7} \frac{\mathrm{d}u}{\mathrm{d}t'} = H' \beta \frac{\mathrm{d}\alpha}{\mathrm{d}t'},$$

$$\frac{1}{T} \frac{\mathrm{d}T}{\mathrm{d}t'} + \frac{1}{\rho} \frac{\mathrm{d}\rho}{\mathrm{d}t'} + \frac{\beta}{1 + \alpha\beta} \frac{\mathrm{d}\alpha}{\mathrm{d}t'} = \frac{M_1}{T\rho(1 + \alpha\beta) R} \frac{\mathrm{d}P}{\mathrm{d}t'}$$

where $$H' = h_1(T) - 2h_2(T) - E_D$$

and $$S = \beta(1 - \alpha) Cp_1(T) + 2\alpha\beta Cp_2(T) + (1 - \beta) Cp_3(T),$$

Cp_i being the mole-specific heat of species i at temperature T.

Algebraic manipulation of these equations yield the following relation between $\mathrm{d}T/\mathrm{d}t'$ and $\mathrm{d}\alpha/\mathrm{d}t'$:

$$\frac{\mathrm{d}T}{\mathrm{d}t'} = \frac{H'A - Tu}{u(1 + \alpha\beta) + SA} \beta \frac{\mathrm{d}\alpha}{\mathrm{d}t'} \tag{A 3}$$

where $$A = \frac{P_1 + \rho_1 u_1^2}{R\rho_1 u_1} - \frac{2u}{R}.$$

The differential equation for the degree of dissociation α (see appendix I) may be written in shock fixed coordinates as follows

$$\frac{\mathrm{d}\alpha}{\mathrm{d}t'} = \frac{\beta\rho_1 u_1^2}{M_1 R_1 u^2}\left[\frac{1-\alpha}{T}K_p - \frac{4\beta\rho_1 u_1 R\alpha^2}{M_1 u}\right]\left[k_{-1}(1-\alpha) + 2k_{-2}\alpha + \frac{1-\beta}{\beta}k_{-3}\right]. \quad \text{(A 4)}$$

This pair of differential equations defines the dissociation and temperature profiles provided the velocity u is replaced by the positive root of the quadratic equation

$$2\times 10^7 J\,(H+\Delta E) + u^2 = u_1^2 = W^2$$

where H is evaluated at temperature T.

The integration was performed using a Runge–Kutta type process due to Scraton (1964) with the initial conditions $\alpha = 0, T = T_0$ at $t' = 0$. The values of T_0 and u_1 may be computed from the conditions in front of the shock and the equilibrium temperature T_e as shown in appendix II.

Appendix IV. The estimation of parameters in non-linear situations

Since the differential equations (A 3) and (A 4) may be integrated numerically we can assume that the temperature–time profile is given by

$$\phi = f(\mathbf{b}, t'),$$

where the vector $\mathbf{b}$ has components equal in turn to A_{-1}, A_{-2}, A_{-3} and n_{-1}, n_{-2}, n_{-3}. The problem is to find an estimate of $\mathbf{b}$ for which the sum of squares

$$\phi = \sum_{i=1}^{m}(T_i - \theta_i)^2$$

is a minimum, where T_i are the experimental temperatures and θ_i are the predicted temperatures.

One approach to this problem is to differentiate ϕ with respect to each parameter, set the result to zero and solve the resulting equations. However, when the model is non-linear in the parameters these equations are non-linear and so an iterative technique must be used. The equations are linearized by expanding the model in a Taylor series about the current estimate $\mathbf{b}^0$ (retaining only first order terms). This leads to an improved estimate $\mathbf{b}$ $(=\mathbf{b}^0+\boldsymbol{\delta}_l)$ for the linearized model, where $\boldsymbol{\delta}_l$ is the solution of

$$A\boldsymbol{\delta}_l = \mathbf{g},$$

where $A = P'P$, $\mathbf{g} = P'\{y - f_{b\simeq b_0}\}$, P being then $n\times k$ matrix with elements $(\partial f_i/\partial b_j)_{b=b_0}$. If the point b is an improvement over the point $\mathbf{b}_0$ for the non-linear model, in the sense of having a smaller sum of squares, the repeated application of this procedure will lead to a solution of the problem. If not, the Taylor series method does not converge. However, it is always possible to obtain a smaller sum of squares by moving in the steepest descent direction δ_g, which has components $\{-\partial\phi/\partial b_j\}$ in the parameter space. Methods based entirely on the steepest descent direction have not been successful since they take a very large number of iterations.

PROCEEDINGS OF THE ROYAL SOCIETY A MATHEMATICAL, PHYSICAL & ENGINEERING SCIENCES

Marquardt's idea is that the best direction to move in lies between the Taylor series direction $\boldsymbol{\delta}_t$ and the steepest descent direction $\boldsymbol{\delta}_g$. He finds this direction $\boldsymbol{\delta}$ and the distance along it by solving the equations

$$(A + \lambda I)\,\boldsymbol{\delta} = \mathbf{g}.$$

When $\lambda = 0$, $\boldsymbol{\delta}$ is the Taylor series direction and as λ increases $\boldsymbol{\delta}$ swings towards the steepest descent direction $\boldsymbol{\delta}_g$. Marquardt's strategy contains two further ideas. Within an iteration λ is increased until a reduced sum of squares is obtained. Between iterations λ is successively reduced so that as the minimum is reach $\boldsymbol{\delta}$ swings towards the Taylor series direction. This ensures that his algorithm has second-order convergence near the minimum.

References

Amdur, I. 1935 *J. Am. Chem. Soc.* **57**, 856.

Amdur, I. 1938 *J. Am. Chem. Soc.* **60**, 2347.

Amdur, I. & Robinson, A. L. 1933 *J. Am. Chem. Soc.* **55**, 1395, 2615.

Bennett, J. E. & Blackmore, D. R. 1968 *Proc. Roy. Soc.* A **305**, 553.

Bulewicz, E. M. & Sugden, T. M. 1958 *Trans. Faraday Soc.* **54**, 1855.

Dixon-Lewis, A., Sutton, M. M. & Williams, A. 1962 *Discuss. Faraday Soc.* **33**, 205.

Dixon-Lewis, A., Sutton, M. M. & Williams, A. 1965 *Tenth Symposium* (*Int.*) *on Combustion*, p. 495. Cambridge, England: Combustion Institute.

Gardiner, W. C. & Kistiakowsky, G. B. 1961 *J. Chem. Phys.* **35**, 1765.

Gaydon, A. G. & Hurle, I. R. 1961 *Proc. Roy. Soc.* A **262**, 38.

Gaydon, A. G. & Hurle, I. R. 1962 *Eighth Symposium* (*Int.*) *on Combustion*, p. 309. Baltimore: Williams & Wilkins.

Gaydon, A. G. & Hurle, I. R. 1963 *The shock tube in high-temperature physics.* London: Chapman and Hall; New York: Reinhold.

Halstead, C. J. & Jenkins, D. R. 1968 To be published in the Proceedings of the Twelfth Symposium (Int.) on Combustion.

Hurle, I. R. 1964 *J. Chem. Phys.* **41**, 3911.

Hurle, I. R. 1967*a* *Reports on progress in physics* **30**, part 1, p. 149. London: Institute of Physics and the Physical Society.

Hurle, I. R. 1967*b* *Eleventh Symposium* (*Int.*) *on Combustion*, p. 827. Berkeley, California: Combustion Institute.

Hurle, I. R. Mackey, P. & Rosenfeld, J. L. J. 1968 *Ber. Bunsen- Ges. phys. Chem.* **72**, 991.

Jacobs, T. A. Giedt, R. R. & Cohen, N. 1967 *J. Chem. Phys.* **47**, 54.

Jenkins, D. R. 1966 *Proc. Roy. Soc.* A **293**, 493.

Kiefer, J. H. & Lutz, R. W. 1967 *J. Chem. Phys.* **47**, 54.

Larkin, F. S. & Thrush, B. A. 1964 *Discuss. Faraday Soc.* **37**, 112.

Larkin, F. S. & Thrush, B. A. 1965 *Tenth Symposium* (*Int.*) *on Combustion* p. 1397. Cambridge, England: Combustion Institute.

Marquardt, D. W. 1963 *SIAM J.* **11**, 2, 431.

Marquardt, D. W. 1966 *SHARE program Library*, Distn. no. SDA 3094 (Revised).

Miscellaneous contributors 1962 *Proc. Solvay Conf. on Transfert d'Energie dans les Gaz.* New York: Interscience.

Patch, R. W. 1962 *J. Chem. Phys.* **36**, 1919.

Rink, J. P. 1962 *J. Chem. Phys.* **36**, 262.

Rosenfeld, J. L. J. & Sugden, T. M. 1964 *Combust. Flame* **8**, 37.

Schott, G. L. & Bird, P. F. 1964 *J. Chem. Phys.* **41**, 1869.

Scraton, R. E. 1964 *Computer J.* **7** 3, 246.

Sutton, E. A. 1962 *J. Chem. Phys.* **36**, 1923.

PROCEEDINGS OF THE ROYAL SOCIETY A MATHEMATICAL, PHYSICAL & ENGINEERING SCIENCES